

FINAL ASSIGNMENT

FINITE ELEMENT METHODS IN FLUIDS

- SANATH KESHAV

1 Transport Problem

The actin filaments and monomers densities (F and G) are modelled by the following coupled system of partial differential equations

$$\frac{\partial F}{\partial t} = -u \cdot \nabla F + D_F \nabla^2 F - \sigma_F F \quad (1)$$

$$\frac{\partial G}{\partial t} = D_G \nabla^2 G - \sigma_G + \sigma_{GF} F \quad (2)$$

where $u(x, y) = \frac{-1}{1500}(rx, ry) \mu m/s$ and $r = \sqrt{x^2 + y^2}$. A dirichlet boundary condition $F(r = 25) = 80 \mu m$ is imposed and no flux neumann boundary condition is imposed for the rest of the boundary for F and everywhere for G .

The two PDEs can be solved either in a monolithic fashion or a staggered fashion. Since the PDE involving F does not contain G, the two PDEs can be solved in a decoupled staggered way which is also computationally cheaper because it would involve solving two smaller systems of linear equations instead of one big system of linear equations.

In order to solve the PDEs, we use a Crank Nicolson discretization in the temporal direction and Linear Galerkin elements in space. The choice of crank nicolson can be justified by its unconditional stability which would allow us to use coarser time steps as well as second order accuracy in time. We can also observe that our convection velocity is much smaller in order compared to the diffusion coefficient, hence making it a diffusion dominated problem. We can conclude that there is no need for stabilization. We also know that the crank nicolson scheme shows excellent properties of numerical damping and phase error for low peclet numbers.

As an example the problem is solved on a mesh which is discretized with 20 elements in the radial direction and 10 elements in the tangential direction shown below.

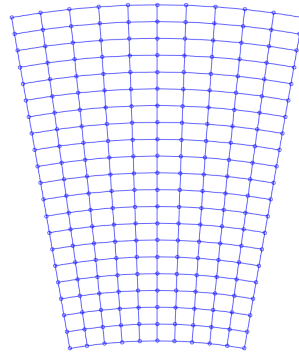


Fig 1. Mesh $[N_R \times N_\theta] = [20 \times 10]$

1.1 Temporal Discretization

$$\begin{aligned}
F_t &= -u \cdot \nabla F + D_F \nabla^2 F - \sigma_F F \\
\frac{F^{n+1} - F^n}{\Delta t} &= \theta F_t^{n+1} + (1 - \theta) F_t^n \\
\frac{\Delta F}{\Delta t} - \theta \Delta F_t^{n+1} &= F_t^n \quad \text{where } \Delta F = F^{n+1} - F^n
\end{aligned}$$

$$\frac{\Delta F}{\Delta t} + \theta(u \cdot \nabla) \Delta F - \theta D_F \nabla^2 \Delta F + \theta \sigma_F \Delta F = u \cdot \nabla F^n + D_F \nabla^2 F^n - \sigma_F F^n \quad (3)$$

Similarly,

$$\begin{aligned}
G_t &= D_G \nabla^2 G - \sigma_G + \sigma_{GF} F \\
\frac{G^{n+1} - G^n}{\Delta t} &= \theta G_t^{n+1} + (1 - \theta) G_t^n \\
\frac{\Delta G}{\Delta t} - \theta \Delta G_t^{n+1} &= G_t^n \quad \text{where } \Delta G = G^{n+1} - G^n
\end{aligned}$$

$$\frac{\Delta G}{\Delta t} - \theta D_G \nabla^2 \Delta G + \theta \sigma_G \Delta G = D_G \nabla^2 G^n - \sigma_G G^n + \sigma_{GF} F^n + \theta \sigma_{GF} \Delta F \quad (4)$$

1.2 Spatial Discretization

Let us multiply a test function w and integrate over the domain.

$$\begin{aligned}
(w, \frac{\Delta F}{\Delta t}) + \theta(w, (u \cdot \nabla) \Delta F) - \theta D_F(w, \nabla^2 \Delta F) + \theta \sigma_F(w, \Delta F) &= \dots \\
(w, u \cdot \nabla F^n) + D_F(w, \nabla^2 F^n) - \sigma_F(w, F^n) &
\end{aligned}$$

Integration by parts and ignoring the boundary integrals due to zero flux boundary condition on Γ_N and $w = 0$ on Γ_D

$$\begin{aligned}
(w, \frac{\Delta F}{\Delta t}) + \theta(w, (u \cdot \nabla) \Delta F) + \theta D_F(\nabla w, \nabla \Delta F) + \theta \sigma_F(w, \Delta F) &= \dots \\
(w, u \cdot \nabla F^n) - D_F(\nabla w, \nabla F^n) - \sigma_F(w, F^n) &
\end{aligned}$$

$$\left(\frac{1}{\Delta t} \mathbf{M} + \theta \mathbf{C} + \theta D_F \mathbf{K} + \theta \sigma_F \mathbf{M} \right) \Delta F = (\mathbf{C} - D_F \mathbf{K} - \sigma_F \mathbf{M}) F^n \quad (5)$$

Similarly for Eq. 4,

$$\begin{aligned}
(w, \frac{\Delta G}{\Delta t}) - \theta D_G(w, \nabla^2 \Delta G) + \theta \sigma_G(w, \Delta G) &= \dots \\
D_G(w, \nabla^2 G^n) - \sigma_G(w, G^n) + \sigma_{GF}(w, F^n) + \theta \sigma_{GF}(w, \Delta F) &
\end{aligned}$$

Integration by parts and ignoring the boundary integrals due to zero flux boundary condition on Γ_N

$$\begin{aligned}
(w, \frac{\Delta G}{\Delta t}) + \theta D_G(\nabla w, \nabla \Delta G) + \theta \sigma_G(w, \Delta G) &= \dots \\
D_G(\nabla w, \nabla G^n) - \sigma_G(w, G^n) + \sigma_{GF}(w, F^n) + \theta \sigma_{GF}(w, \Delta F) &
\end{aligned}$$

$$\left(\frac{1}{\Delta t}\mathbf{M} + \theta D_G \mathbf{K} + \theta \sigma_G \mathbf{M}\right) \Delta G = \left(-D_G \mathbf{K} - \sigma_G \mathbf{M}\right) G^n + \left(\sigma_{\hat{G}F} \mathbf{M}\right) F^n + \left(\theta \sigma_{\hat{G}F} \mathbf{M}\right) \Delta F \quad (6)$$

where,

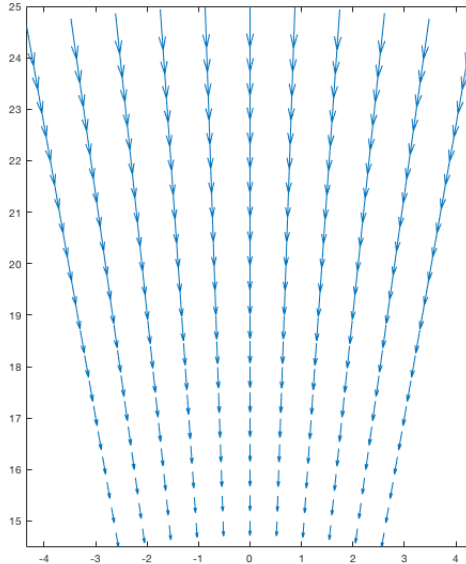
$$\begin{aligned} (w, v) &\rightarrow \mathbf{M} & M_{ab} &= \int_{\Omega} N_a N_b d\Omega \\ (\nabla w, \nabla v) &\rightarrow \mathbf{K} & K_{ab} &= \int_{\Omega} \nabla N_a \cdot \nabla N_b d\Omega \\ (u \cdot \nabla w, v) &\rightarrow \mathbf{C} & C_{ab} &= \int_{\Omega} N_b (u \cdot \nabla N_a) d\Omega \end{aligned}$$

1.3 Numerical results

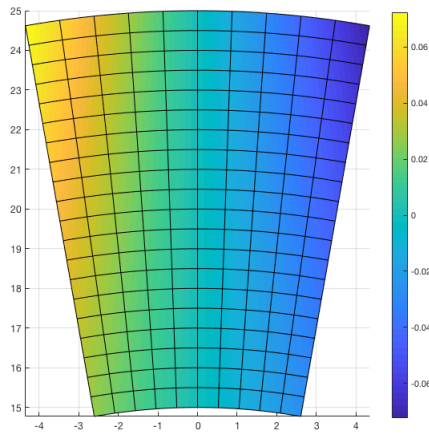
Eq. 5 and 6 are solved at each time step to obtain the evolution of the variables F and G in time. Initial condition is taken as 0 on Ω except the dirichlet boundary Γ_D for both F and G. The following parameters are considered for the results presented.

$$\begin{aligned} D_F &= 5 \mu m/s & \sigma_F &= 0.25 s^{-1} \\ D_G &= 15 \mu m/s & \sigma_G &= 2 s^{-1} & \sigma_{\hat{G}F} &= 0.5 s^{-1} \\ F(r=25) &= 80 \mu M & [N_R \times N_\theta] &= [20 \times 10] \\ t_{final} &= 0.5 s & \text{No of time steps} &= 50 \end{aligned}$$

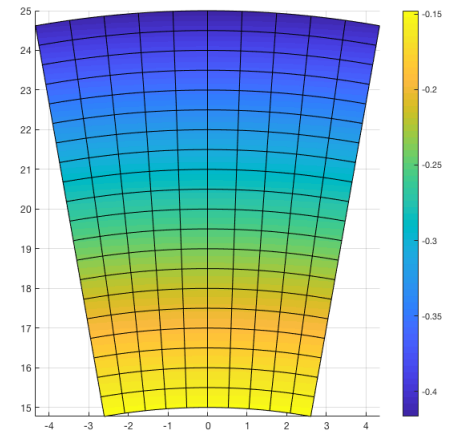
Convection velocity given by $u(x, y) = \frac{-1}{1500}(rx, ry) \mu m/s$ and $r = \sqrt{x^2 + y^2}$. θ is chosen to be 0.5 in order to obtain second order accuracy in time. θ can also be chosen to be 0, 1, or $\frac{2}{3}$ in order to solve the problem using forward euler, backward euler and galerkin method respectively but at the cost of only first order accuracy in time.



Convection velocity $u(x, y) = \frac{-1}{1500}(rx, ry) \mu m/s$ Quiver plot



Convection X velocity function



Convection Y velocity function

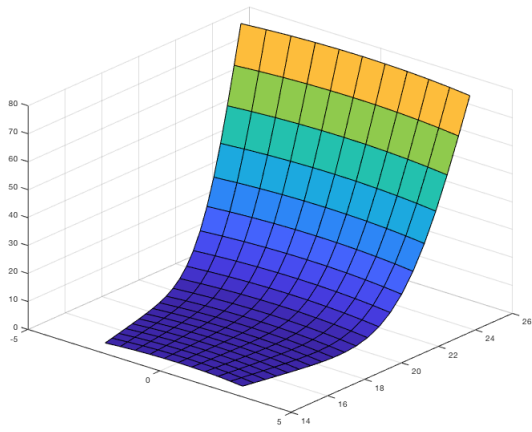


Fig 2a: Final F

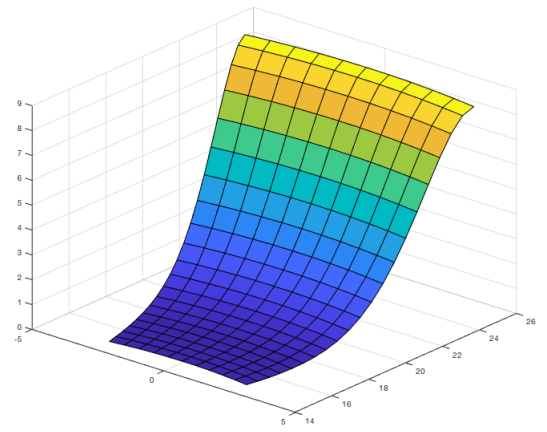


Fig 2b: Final G

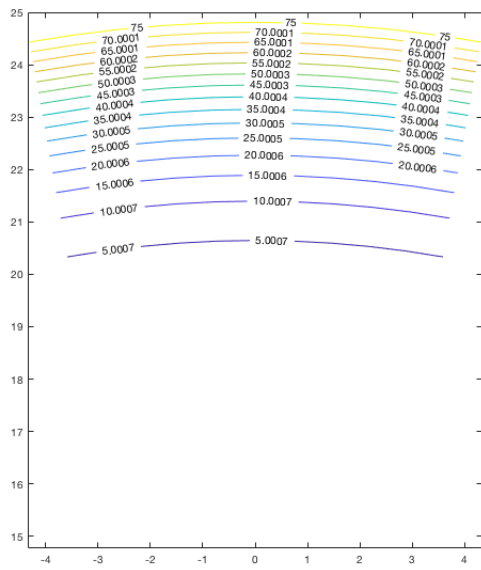


Fig 2c: Final F Contour

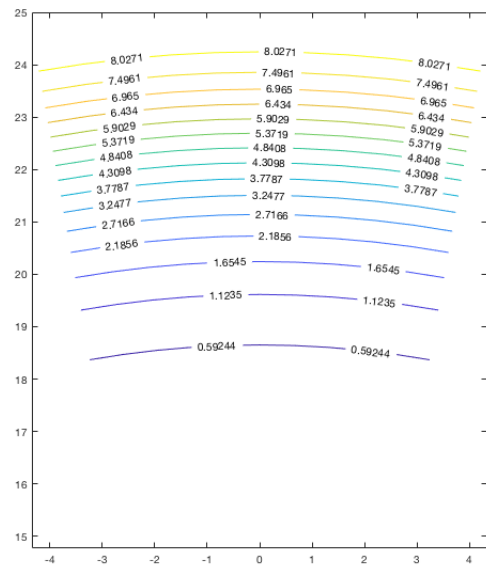


Fig 2d: Final G Contour

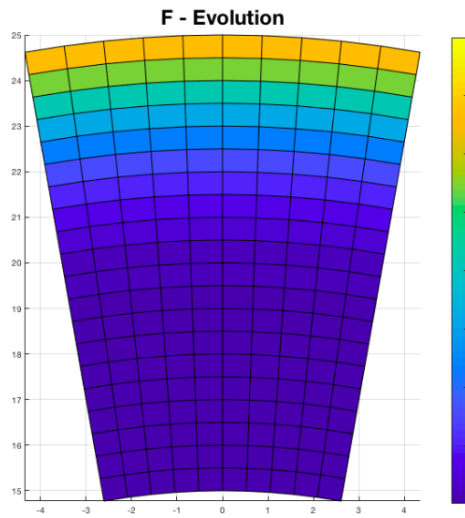


Fig 2e: Final F

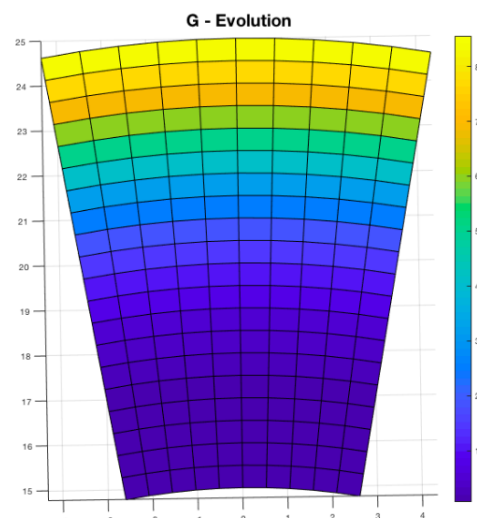


Fig 2f: Final G

The X velocity, Y velocity and the quiver plot of the convection velocity function $u(x, y) = \frac{-1}{1500}(rx, ry)$ were plotted. The final F and G densities and their contours corresponding to the convective velocity are plotted. It was observed that the dirichlet boundary condition $F(r = 25) = 80$ is imposed correctly and also visually it can be observed that the slope of the function on the boundaries where the zero flux condition is imposed equals 0.

2 Stokes Problem

Consider the general stokes problem given by

$$\begin{aligned}
 -\nabla \cdot \sigma &= b && \text{in } \Omega \text{ (Equilibrium)} \\
 \nabla \cdot v &= 0 && \text{in } \Omega \text{ (Incompressibility)} \\
 v &= v_D && \text{on } \Gamma_D \text{ (Dirichlet BC)} \\
 n \cdot \sigma &= t && \text{on } \Gamma_N \text{ (Neumann BC)} \\
 \sigma &= -pI + 2\mu \nabla^s v && \text{(Linear Stokes law)}
 \end{aligned}$$

with prescribed velocity boundary conditions at $r = 15$ and $r = 25$ and zero traction boundary condition everywhere else.

$$\begin{aligned}
 u_r(r = 15) &= -0.15 & u_\theta(r = 15) &= 0 \\
 u_r(r = 25) &= -0.30 & u_\theta(r = 25) &= 0
 \end{aligned}$$

Since we intend to impose the zero traction boundary condition exactly, let us formulate in terms of **cauchy stress** rather than in terms of velocity and pressure. Let us multiply a test function w and integrate over the domain.

$$\begin{aligned}
 - \int_{\Omega} w \cdot \nabla \cdot \sigma d\Omega &= \int_{\Omega} w \cdot b d\Omega \\
 \int_{\Omega} q \nabla \cdot v d\Omega &= 0
 \end{aligned}$$

Using Greens theorem we get,

$$\begin{aligned}
 \int_{\Omega} \nabla w : \sigma d\Omega - \int_{\partial\Omega} w \cdot \sigma \cdot n^0 d\Gamma &= \int_{\Omega} w \cdot b d\Omega \\
 \int_{\Omega} \nabla w : (-pI + 2\mu \nabla^s v) d\Omega &= \int_{\Omega} w \cdot b d\Omega \\
 - \int_{\Omega} p \nabla \cdot w d\Omega + \int_{\Omega} 2\mu \nabla w : \nabla^s v d\Omega &= \int_{\Omega} w \cdot b d\Omega
 \end{aligned}$$

The equations that are going to be solved are

$$2\mu \int_{\Omega} \nabla^s w : \nabla^s v d\Omega - \int_{\Omega} p \nabla \cdot w d\Omega = \int_{\Omega} w \cdot b d\Omega \quad (7)$$

$$\int_{\Omega} q \nabla \cdot v d\Omega = 0 \quad (8)$$

They can be rewritten as

$$a(w, v) + b(w, p) = (w, b) \quad \forall w \in \mathcal{V} \quad (9)$$

$$b(v, q) = 0 \quad \forall q \in \mathcal{Q} \quad (10)$$

$$\begin{bmatrix} \mathbf{K} & \mathbf{G} \\ \mathbf{G}^T & \mathbf{0} \end{bmatrix} \begin{bmatrix} \mathbf{u} \\ \mathbf{p} \end{bmatrix} = \begin{bmatrix} \mathbf{f} \\ \mathbf{h} \end{bmatrix}$$

2.1 Imposing Essential (Dirichlet) Boundary conditions

Since the dirichlet boundary conditions are prescribed in polar coordinates, they have to be transformed to Cartesian coordinates and then prescribed.

$$\begin{aligned}
 x &= r\cos\theta & y &= r\sin\theta & r &= \sqrt{x^2 + y^2} \\
 \theta &= \tan^{-1}\frac{y}{x} & v_r &= \dot{r} & v_\theta &= r\dot{\theta} \\
 v_x &= \frac{dx}{dt} = \dot{r}\cos\theta - r\dot{\theta}\sin\theta & v_y &= \frac{dy}{dt} = \dot{r}\sin\theta + r\dot{\theta}\cos\theta \\
 v_x &= v_r\cos\theta - v_\theta\sin\theta & v_y &= v_r\sin\theta + v_\theta\cos\theta \\
 \begin{bmatrix} v_x \\ v_y \end{bmatrix} &= \begin{bmatrix} \cos\theta & -\sin\theta \\ \sin\theta & \cos\theta \end{bmatrix} \begin{bmatrix} v_r \\ v_\theta \end{bmatrix}
 \end{aligned}$$

The dirichlet boundary conditions that were imposed are

$$\begin{aligned}
 v_x(r = 25) &= (-0.30)\frac{x}{\sqrt{x^2 + y^2}} & v_y(r = 25) &= (-0.30)\frac{y}{\sqrt{x^2 + y^2}} \\
 v_x(r = 15) &= (-0.15)\frac{x}{\sqrt{x^2 + y^2}} & v_y(r = 15) &= (-0.15)\frac{y}{\sqrt{x^2 + y^2}}
 \end{aligned}$$

2.2 Verification of solver

The results are presented for the problem solved using Q_2Q_1 LBB stable elements where the velocity is approximated using quadratic finite elements and pressure is approximated using linear finite elements. The GLS stabilization was also implemented which allows us to use non LBB stable elements like Q_1Q_1 or P_1P_1 elements.

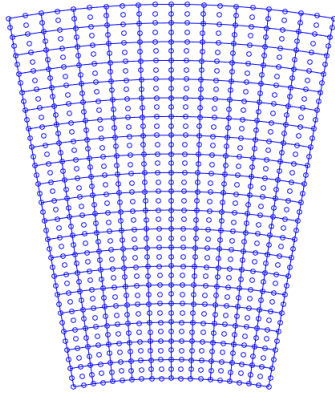


Fig 3a: Q2 Mesh for Velocity

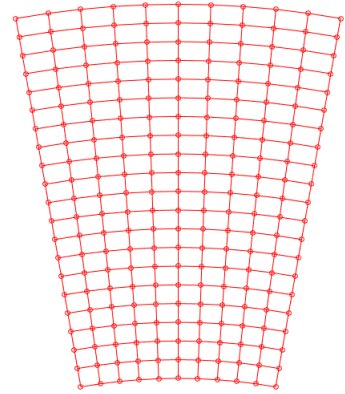


Fig 3b: Q1 Mesh for Pressure

The correctness of the solver employed was verified by performing an order of convergence analysis on a problem with a priori known exact solution. The L^2 error of the pressure, L^2 error of the velocity and the H^1 semi-norm error of the velocity were computed successively with refinement. The error versus the element size were plotted on a logarithmic scale.

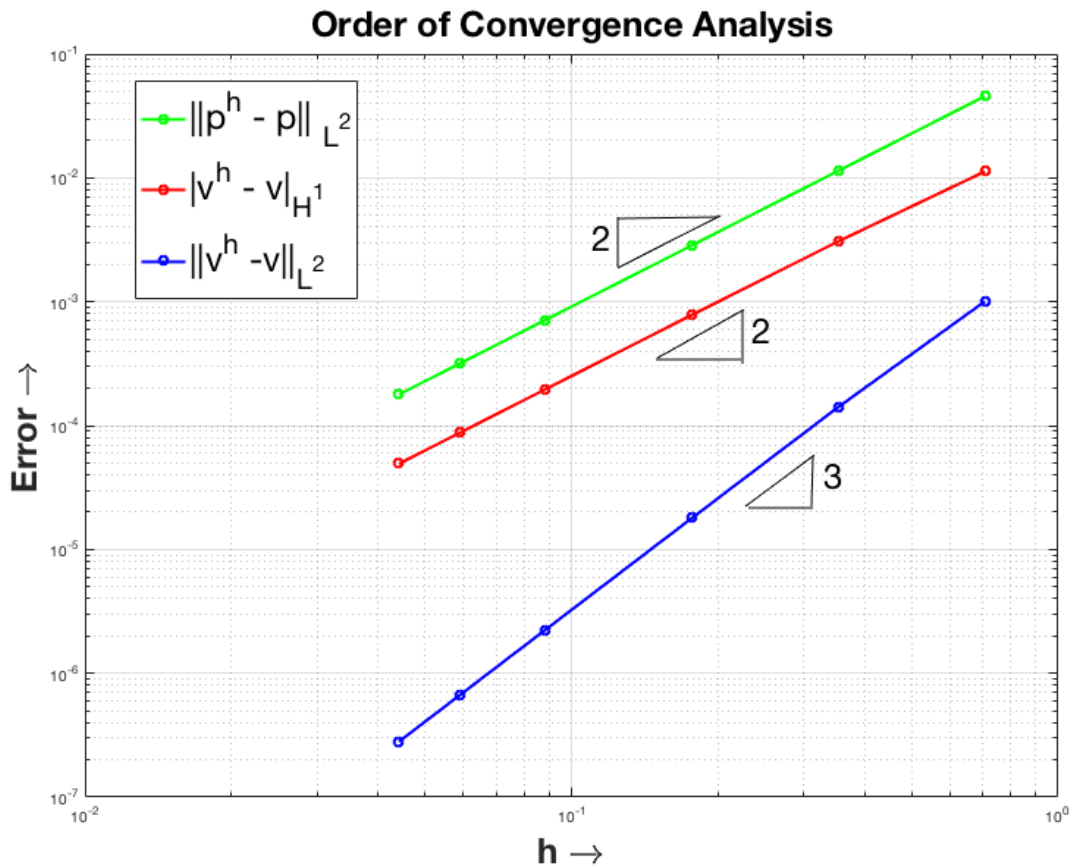


Fig 4. Order of Convergence

Expected order of 3 was observed for L^2 error of the velocity because of the use of Q_2 elements to interpolate velocity. Expected order of 2 was observed for H^1 semi-norm error of the velocity and expected order of 2 was observed for L^2 error of the pressure because of the use of Q_1 elements to interpolate pressure.

1.999635493524672	1.873302176674072	2.832325805975174
2.000330546619946	1.973753558430197	2.978879222764457
2.000030956597092	1.993369649775693	2.996589698011148
2.000003845615942	1.997883037101279	2.999112251694083
2.000001108133545	1.998952202313913	2.999587524766460
L^2 norm Pressure	H^1 semi norm Velocity	L^2 norm Velocity

2.3 Numerical Results

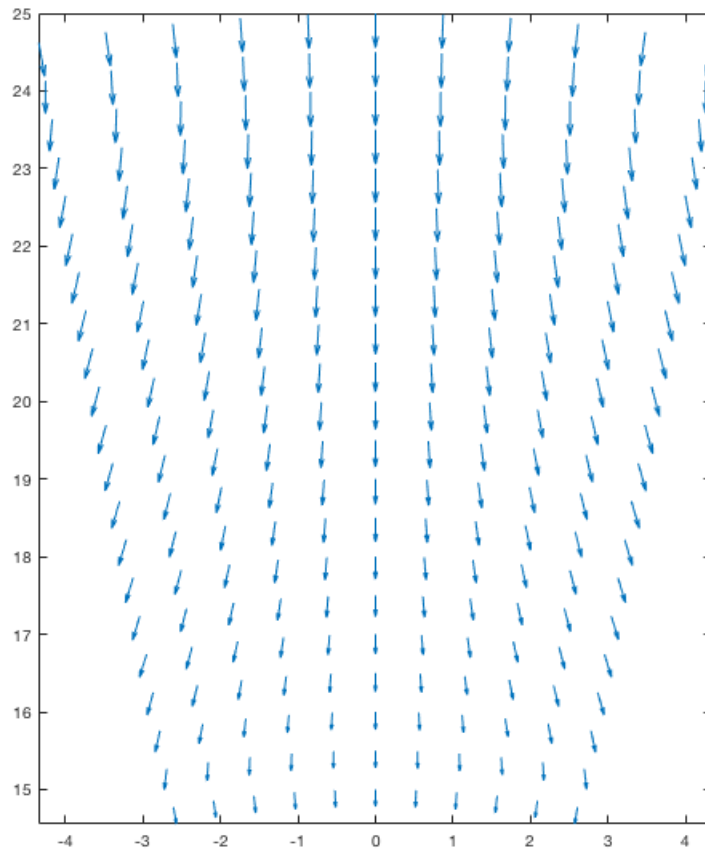


Fig 5. Velocity profile

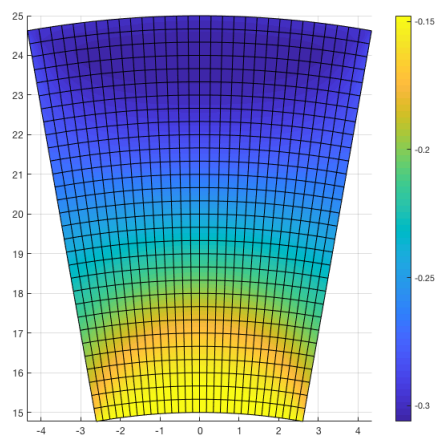


Fig 6a: Y Velocity

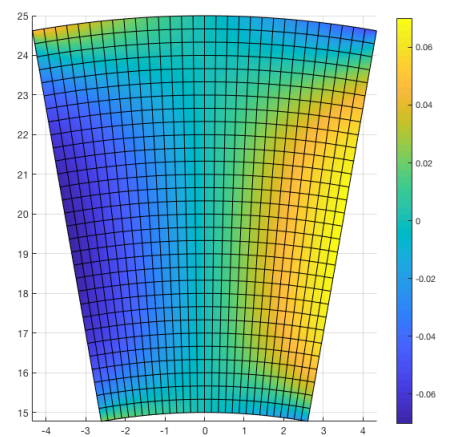


Fig 6b: X Velocity

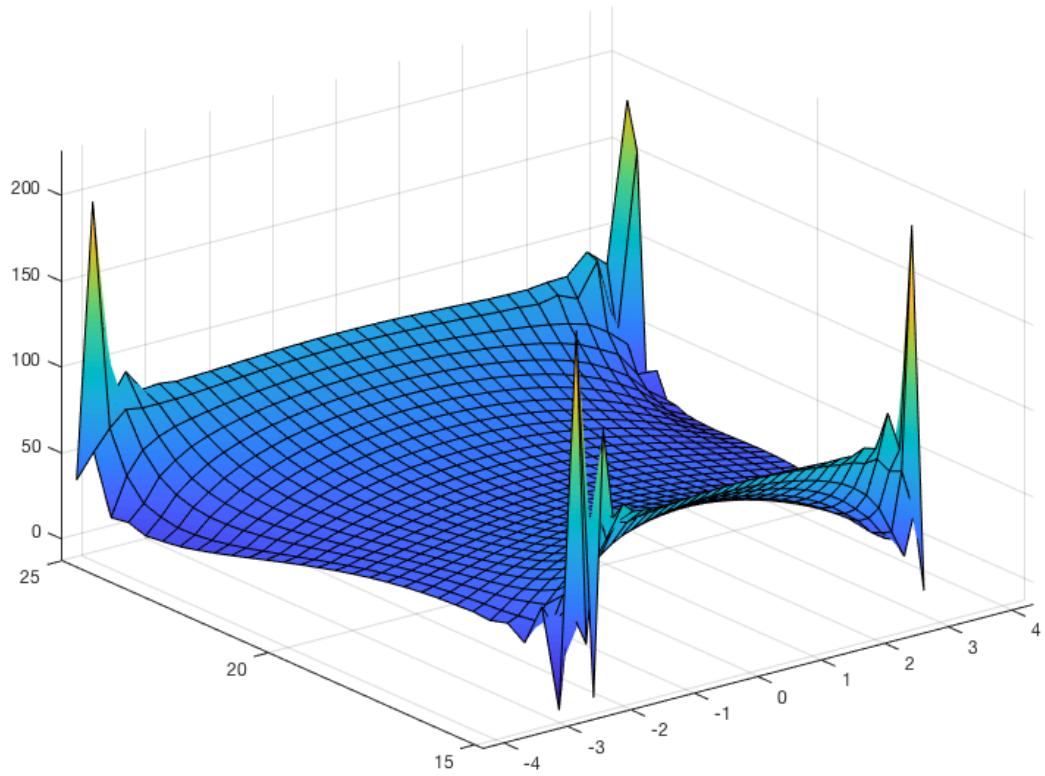


Fig 7. Pressure profile

$$\begin{bmatrix} v_r \\ v_\theta \end{bmatrix} = \begin{bmatrix} \cos\theta & \sin\theta \\ -\sin\theta & \cos\theta \end{bmatrix} \begin{bmatrix} v_x \\ v_y \end{bmatrix} \quad (11)$$

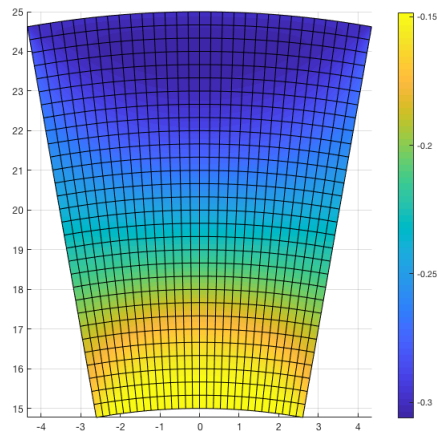


Fig 8a: Radial Velocity

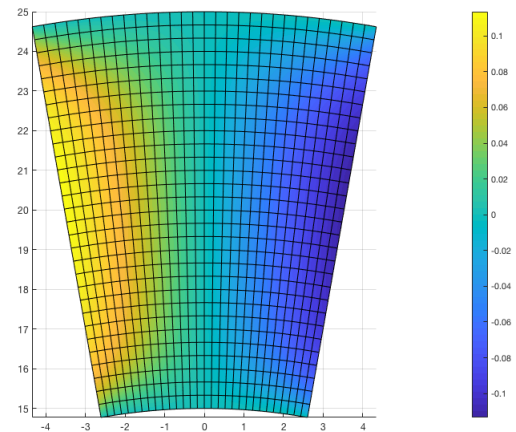


Fig 8b: Tangential Velocity

The X velocity, Y velocity and the quiver plot of the velocity profiles were plotted. The radial and the tangential components of the velocity were computed from the X and Y velocity to ensure that the boundary conditions at $r = 25$ and $r = 15$ are correctly imposed. Computed pressure was visualized. It was observed that the pressure reached a high value in the corners and hence it would be better to go for adaptive meshing towards the corners.

3 Coupled Problem

The equations governing the coupled flow are given by

$$\nu \nabla \cdot (\nabla^s u) + \nabla \cdot \sigma_m(F) + T_m(u) = 0 \quad \text{in } (0, T) \times \Omega \quad (12)$$

$$\frac{\partial F}{\partial t} = -u \cdot \nabla F + D_F \nabla^2 F - \sigma_F F \quad \text{in } (0, T) \times \Omega \quad (13)$$

$$\frac{\partial G}{\partial t} = D_G \nabla^2 G - \sigma_G + \sigma_{\hat{G}F} F \quad \text{in } (0, T) \times \Omega \quad (14)$$

with the dirichlet boundary conditions are

$$\begin{aligned} v_x(r = 25) &= (-0.30) \frac{x}{\sqrt{x^2 + y^2}} & v_y(r = 25) &= (-0.30) \frac{y}{\sqrt{x^2 + y^2}} \\ v_x(r = 15) &= (-0.15) \frac{x}{\sqrt{x^2 + y^2}} & v_y(r = 15) &= (-0.15) \frac{y}{\sqrt{x^2 + y^2}} \\ & & F(r = 25) &= 80 \mu m \end{aligned}$$

and traction is zero everywhere else for u and no flux boundary condition everywhere else for F and G .

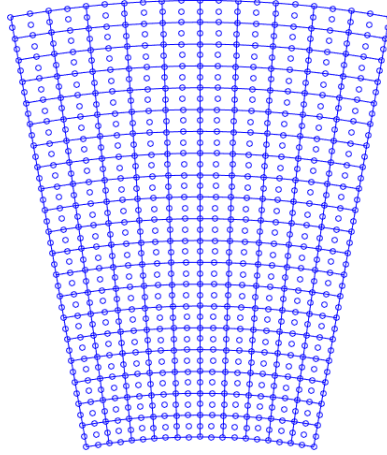


Fig 9. Q₂ elements for interpolating u, F, G

Equations 13 and 14 are discretized in time using Crank Nicolson method and Galerkin method in space. The weak form is given by the following. Refer to Section 1.2 for the detailed derivation.

$$\left(w, \frac{\Delta F}{\Delta t}\right) + \theta \left(w, (u \cdot \nabla) \Delta F\right) + \theta D_F (\nabla w, \nabla \Delta F) + \theta \sigma_F(w, \Delta F) = \left(w, u \cdot \nabla F^n\right) - D_F (\nabla w, \nabla F^n) - \sigma_F(w, F^n)$$

$$\left(w, \frac{\Delta G}{\Delta t}\right) + \theta D_G (\nabla w, \nabla \Delta G) + \theta \sigma_G(w, \Delta G) = D_G (\nabla w, \nabla G^n) - \sigma_G(w, G^n) + \sigma_{\hat{G}F}(w, F^n) + \theta \sigma_{\hat{G}F}(w, \Delta F)$$

$$\left(\frac{1}{\Delta t} \mathbf{M} + \theta \mathbf{C} + \theta D_F \mathbf{K} + \theta \sigma_F \mathbf{M}\right) \Delta F = \left(\mathbf{C} - D_F \mathbf{K} - \sigma_F \mathbf{M}\right) F^n \quad (15)$$

$$\left(\frac{1}{\Delta t}\mathbf{M} + \theta D_G \mathbf{K} + \theta \sigma_G \mathbf{M}\right) \Delta G = (-D_G \mathbf{K} - \sigma_G \mathbf{M}) G^n + (\sigma_{GF} \mathbf{M}) F^n + (\theta \sigma_{GF} \mathbf{M}) \Delta F \quad (16)$$

Equation 12 is multiplied with a test function w and integrating over the domain Ω

$$\int_{\Omega} w \nu \nabla \cdot (\nabla^s u) d\Omega + \int_{\Omega} w \nabla \cdot \sigma_m(F) d\Omega + \int_{\Omega} w T_m(u) d\Omega = 0$$

Integrating the first and the second term by parts and applying the appropriate boundary conditions,

$$\begin{aligned} - \int_{\Omega} \nabla^s w : \nu \nabla^s u d\Omega - \int_{\Omega} \nabla^s w : \sigma_m(F) d\Omega + \int_{\Omega} w T_m(u) d\Omega &= 0 \\ -\mathbf{K}u + \mathbf{T}_f F + \mathbf{T}_u u &= 0 \\ -\mathbf{K}u + \mathbf{T}_u u &= -\mathbf{T}_f F^* \end{aligned} \quad (17)$$

3.1 Algorithm Employed

```

for time loop — n
.
.
while tolerance on ||F_n(k+1) - F_n(k)||
and ||u_n(k+1) - u_n(k)|| — k
.
Solve Eq 17 to compute u_n(k+1) using F_n(k)
Solve Eq 15 to compute F_n(k+1) using u_n(k+1)
.
end
u_n(n+1) = u_n(k+1)
F_n(n+1) = F_n(k+1)
.
Solve Eq 16 to compute G_n(n+1) using F_n(n+1)
.
end

```

3.2 Numerical Results

The numerical results obtained for $t_{final} = 0.5s$ No of time steps = 50 are presented.

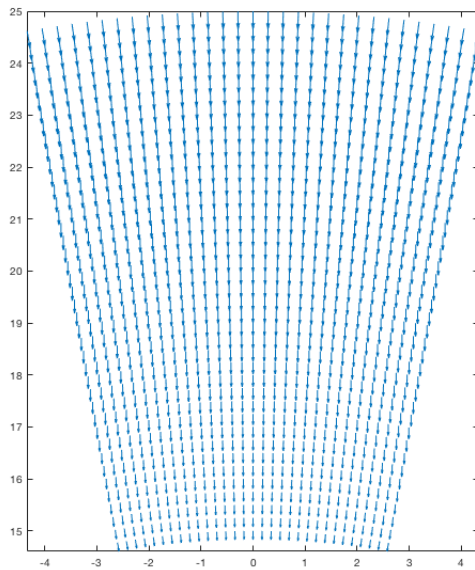


Fig 10 a. Final Velocity profile

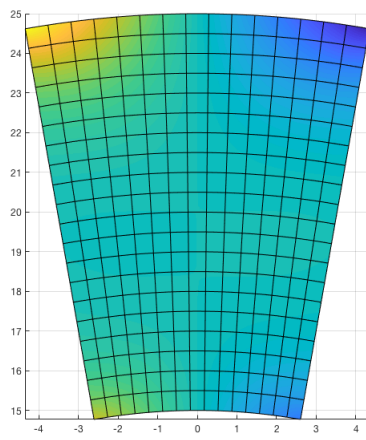


Fig 10 b: Final X Velocity

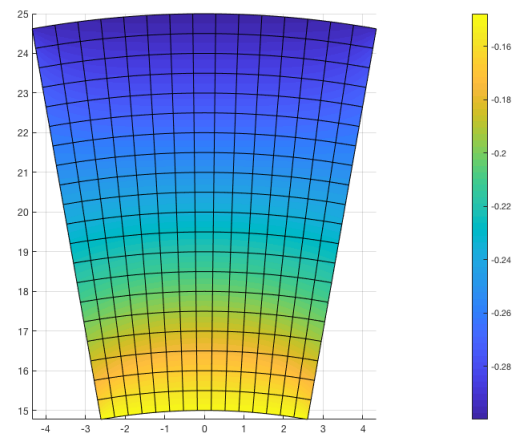


Fig 10 c: Final Y Velocity

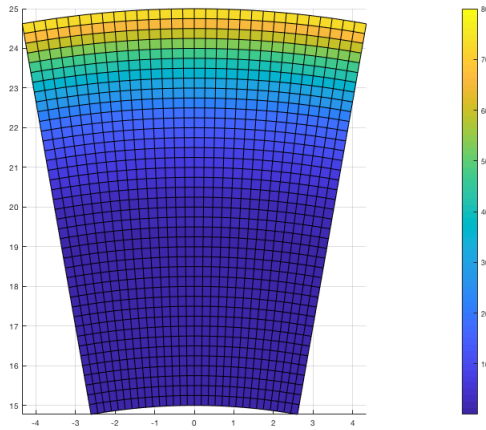


Fig 10 d: Final F density

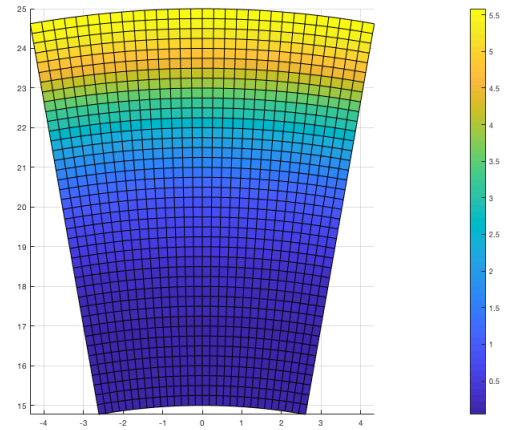


Fig 10 e: Final G density

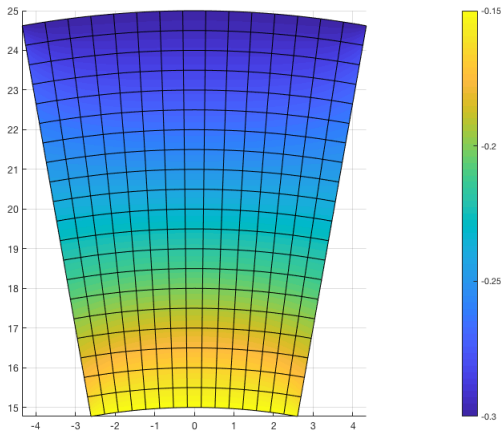


Fig 10 f: Radial Velocity

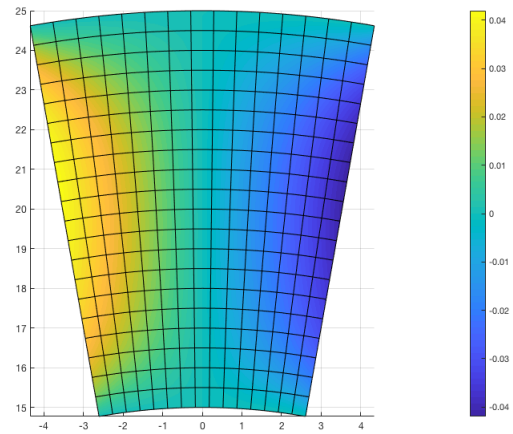


Fig 10 g: Tangential Velocity

The X velocity, Y velocity and the quiver plot of the final velocity profiles were plotted. The final F and G density corresponding to the computed convective velocity are plotted. The radial and the tangential components of the velocity were computed from the X and Y velocity to ensure that the boundary conditions at $r = 25$ and $r = 15$ are correctly imposed.

4 Difficulties and some comments

The behavior of the coupled problem was not able to be reproduced for a lower order linear interpolation of u, F, G for a reason yet to be known. Absence of a known initial condition for F and G densities brings ambiguity into the system. Inability to understand the practical physics of the problem under the given boundary conditions lead to inability of validating the model and the numerical solution of the coupled system. It is clear that much additional work is required before a complete understanding of this problem for myself.

To clone or Download, use git or checkout with SVN using the following web URL for all the codes and supporting files that were developed to solve the three problems.

https://github.com/sanathkeshav/FEF_Final_Assignment.git